ORIGINAL PAPER

Dominant Cutting Parameters Affecting the Specific Energy of Selected Sandstones when Using Conical Picks and the Development of Empirical Prediction Models

Xiang Wang[1,2] · Qing-Feng Wang[1,2] · Yun-Pei Liang[3] · Okan Su[4] · Lin Yang[2]

Abstract
Specific energy is one of the most significant parameters in the process of rock cutting and it has been widely used for evaluating the performance of excavation machines. In this paper, based on rock cutting tests that were conducted on a linear cutting machine (LCM), the effects of relevant cutting parameters and characteristics, including the clearance angle, the cone (tip) angle of conical picks, the rake angle and the cutting depth on specific energy were investigated. Five different conical picks with the cone angles between 60° and 100° were used in the experiments. In addition, five different sandstones with uniaxial compressive strength varying from 17.91 to 85.98 MPa were subjected to cutting tests under different levels of cutting parameters. As a result of the tests, it was found that the clearance angle has a considerable effect on cutting force and specific energy. When it was greater than 10°, mean cutting force increased with the increasing cone angle, yet linearly decreased with the increasing rake angle and attack angle. However, specific energy has no statistical relationship with the attack angle, the rake angle, and the cone angle. It does not vary effectively with the relevant angles. Statistical analyses also indicate that strong relationships exist between the specific energy and the cutting depth in a power function. In this context, a general model of specific energy was proposed, and based on the test data and previous studies, empirical models of specific energy were developed using multiple non-linear regression and principal component regression methods. Besides, the statistical analyses showed a good agreement between the measured and predicted specific energy in unrelieved and relieved cutting modes. In conclusion, some prediction models of roadheader production rates were developed that were based on the models of specific energy. By comparing the results with the literature, it was found that the proposed models are valid in predicting the instantaneous cutting rate of roadheader especially at the cutting depth of 7–9 mm. They can be used for preliminary estimation of the production rate of roadheaders. Thus, it can be claimed that the models can offer effective solutions for the prediction of production rate of roadheaders equipped with conical picks.

✉ Xiang Wang
  mywayok@163.com

1 Chongqing Key Laboratory of Manufacturing Equipment Mechanism Design and Control, Chongqing Technology and Business University, Chongqing 400067, China

2 China Coal Technology Engineering Group Chongqing Research Institute, Chongqing 400039, China

3 State Key Laboratory of Coal Mine Disaster Dynamics and Control, Chongqing University, Chongqing 400044, China

4 Department of Mining and Mineral Extraction, Zonguldak Vocational School, Bulent Ecevit University, 67500 Zonguldak, Turkey

Abbreviations
d	Depth of cut (mm)
FC	Cutting force
FN	Normal force
FC_m	Mean cutting force (N)
ICR	Instantaneous cutting rate (m^3/h)
k	Energy transfer ratio
k_{opt}	Ratio of specific energy in relieved to unrelieved cutting mode
L	Cutting distance (m)
M	Mass of rock chips (kg)
P	Cutting power of the cutting head (kW)
R_σ	Coefficient representing rock strength parameters
SE	Specific energy (kWh/m^3)
SE_u	Specific energy in unrelieved mode

SE_{opt}	Optimum specific energy in relieved mode
σ_c	Uniaxial compressive strength of rock (MPa)
σ_t	Tensile strength of rock (MPa)
ρ	Density of the rock (kg/m^3)
α	Tilt angle
β	Rake angle
γ	Attack angle
θ	Clearance angle
ϕ	Cone angle of the pick

1 Introduction

The cutting performance of excavation machines equipped with various types of cutting picks are influenced by cuttability characteristics of rocks, which are usually expressed in terms of both the specific energy expended during rock cutting and tool forces acting on the picks. The specific energy is defined as the work to excavate a unit volume of a rock and is one of the most significant parameters in the selection of a mechanical excavation system. The cuttability efficiency of the pick is mainly evaluated by the specific energy, as well as tool forces and other rock properties. Many theoretical and experimental studies on specific energy have been carried out so far. Hughes (1972) and Mellor (1972) theoretically demonstrated that specific energy can be predicted through the compressive strength and the secant modulus of the rock. Copur et al. (2003) found that the optimum specific energy decreased with increasing the force index in a power function. Bilgin et al. (2006) showed that optimum specific energy linearly increases with the increasing uniaxial compressive and tensile strengths of the rock based on rock cutting experiments carried out on 22 different rocks and minerals at the cutting depths of 3–10 mm. Tiryaki and Dikmen (2006) found that the texture coefficient, feldspar content, cementation coefficient, effective porosity, and pore volume of the rock had considerable effects on the specific energy of rock cutting. Tumac et al. (2007) demonstrated that there are statistical relationships between specific energy and the Shore hardness of the rock. Balci and Bilgin (2007) suggested that the optimum specific energy of full-scale rock cutting could be predicted by the specific energy of a small-scale rock cutting. Tiryaki (2009) modeled the specific energy based on the physical and mechanical properties of a rock using regression trees and artificial neural networks. Yurdakul et al. (2014) proposed that the compressive, the bending and the point load strengths of the rock are the dominant mechanical parameters affecting the specific energy based on principal component analysis. To sum up, it is easy to find from previous studies that the effects of the physical and mechanical properties of rocks on specific energy have been sufficiently researched by scholars and scientists in this field. However, few researchers have

paid attention to the effects of cutting parameters on specific energy such as the rake angle, the attack angle and depth of cut. Therefore, it is necessary to verify the effects of cutting parameters on the specific energy.

On the other hand, the prediction of specific energy is a strong interest for engineers. Full-scale and small-scale testing machines are the most reliable devices at present to determine the accurate values of specific energy. However, these machines would not be available at every research center since they are not standard test equipment. For practical purposes, empirical models also allow engineers and scientists to predict the specific energy. To date, some prediction models have been developed using single-factor regression analysis (Copur et al. 2003; Bilgin et al. 2006; Tumac et al. 2007; Balci et al. 2004; Gunes et al. 2014), regression trees and artificial neural networks (Tiryaki 2009), and adaptive hybrid intelligence techniques (Yurdakul et al. 2014). However, most of the existing models that proposed to use rock properties and relevant cutting parameters were often overlooked. Although there is much evidence that the depth of cut has a significant effect on the specific energy (Hurt and Evans 1981; Fowell and Ochei 1984; Hurt and McAndrew 1985; Bilgin et al. 2006), it is often ignored in most empirical models due to limited test data. Therefore, it is necessary to develop reliable empirical models for the estimation of the specific energy by considering more cutting parameters.

In this study, the effects of some cutting parameters on the specific energy are first discussed in detail based on experimental tests that were conducted on the linear cutting machine. Then, a general prediction model of the specific energy is proposed by considering the cutting parameters and rock strength. Empirical models of specific energy are then developed using non-linear regression and principle component regression methods based on the data collected from the present and previous experiments. Moreover, the validity of empirical models is discussed by statistical analyses. Based on the empirical models of specific energy, the prediction models of roadheader production rate are also developed and discussed.

2 Dominant Parameters Affecting Specific Energy

It is well known that the performance of rock cutting is closely related to rock properties as well as the cutter and cutting parameters. Based on the test data of linear rock cutting, the effects of relevant parameters on specific energy are discussed in detail. The results serve an important basis for developing empirical prediction models for specific energy.

2.1 Rock Cutting Test Procedure

To carry out rock-cutting tests, five different sandstone blocks were collected from quarries in Sichuan province and Chongqing city, China. All the rock samples used for rock-cutting tests had no bedding planes and joints. The physical and mechanical properties of the rocks, including density, uniaxial compressive strength, Brazilian tensile strength and elasticity modulus were determined according to ISRM (1981) standards, the results of which are listed in Table 1. Uniaxial compressive tests were performed on core samples with a diameter of 50 mm and a length of 100 mm. The loading rate was applied within the range from 0.5 to 1.0 MPa/s. Brazilian tensile strength was also determined using core samples in the diameter of 50 mm. However, the ratio of thickness to diameter of the disc samples varied between 0.5 and 0.7. All the tests were repeated 5–6 times and the mean values were taken to be the final results.

Table 1 Physical and mechanical properties of the rocks tested

Rock name	ρ	σ_c	σ_t	E
Sandstone 1	2.22	17.91 ± 4.18	1.64 ± 0.10	3.00 ± 0.56
Sandstone 2	2.43	79.20 ± 5.43	4.97 ± 0.48	15.94 ± 0.68
Sandstone 3	2.36	52.99 ± 2.08	3.67 ± 0.25	5.07 ± 0.11
Sandstone 4	2.36	59.80 ± 6.14	3.93 ± 0.44	5.50 ± 0.25
Sandstone 5	2.59	85.98 ± 9.33	3.69 ± 0.42	6.31 ± 0.30

ρ is density (g/cm^3), σ_c is uniaxial compressive strength (MPa), σ_t is tensile strength (MPa), E is tangent Young modulus (GPa)

2.1.1 Experimental Rig and Test Procedure

Linear cutting machine (LCM), shown in Fig. 1, was utilized to conduct the cutting tests in relieved and unrelieved cutting modes. The dimensions of LCM are $1265 \times 420 \times 570$ mm in dimensions. The maximum size of rock sample placed to LCM is approximately $150 \times 150 \times 200$ mm.

During the test, the target rock sample is placed in a heavy steel box and the cutting depth of the pick is fixed. The tool forces are measured with a 3D load cell, while the distance of the cutter is monitored by a displacement transducer. The data acquisition system records the forces as the raw data, which are processed using MATLAB software.
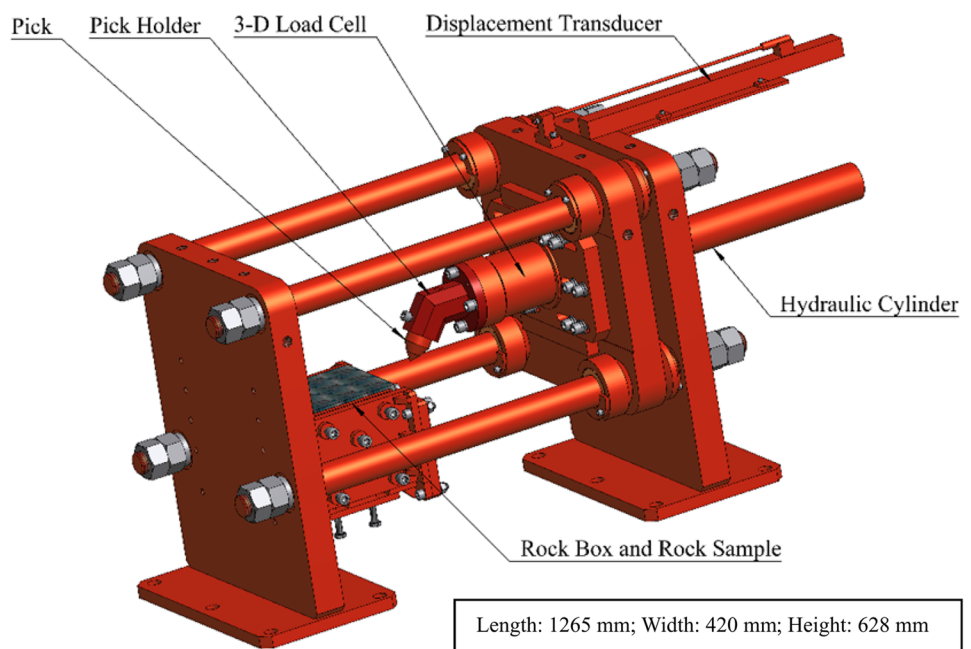
After each test, the chips formed around the conical pick were collected and weighted. From the data of recorded forces and collected chip masses, the specific energy is calculated by Eq. (1).

$$SE = \frac{FC_m L \rho}{3.6M} \times 10^{-6} \tag{1}$$

where, SE is the specific energy (kWh/m^3), FC_m is mean cutting force (N), L is cutting distance (m), ρ is density of the rock (kg/m^3) and M is the mass (kg).

It should be noted that the cutting tests performed close to the edge of the rock were eliminated from the analyses as these tests might give unreliable results and inaccurate rock volume values. Moreover, the rock samples used during the cutting tests have been carefully selected and collected from field. There were no obvious fractures and discontinuity planes within the structure of the samples. Therefore, the measured tool forces and calculated specific energy values

Fig. 1 Schematic view of linear cutting machine (LCM)

Pick   Pick Holder   3-D Load Cell   Displacement Transducer

Hydraulic Cylinder

Rock Box and Rock Sample

Length: 1265 mm; Width: 420 mm; Height: 628 mm

represent a worst case scenario while predicting the instantaneous cutting rate and examining the relationships.

2.1.2 Cutting Ttools and Cutting Parameters

The cone angle and attack angle are the most decisive parameters while selecting an appropriate pick depending on the cutting condition. For example, the picks having higher degree of cone angles greater than 80° can be selected and manufactured for abrasive and hard rocks. As the angle is reduced, the pick would be more suitable for medium-hard rocks and coal. Five conical picks with different geometrical parameters shown in Fig. 2a were manufactured for the cutting experiments in this study. The tip radius of the pick is about 1 mm. The cone angle of conical picks changes between 60° and 100° and their tip diameters are about 22 mm. Accordingly, the attack angle varied from 40° to 60° by changing the pick holders, as shown in Fig. 2b. The main material of pick body is made of steel with medium carbon content while the pick tip is made of carbide alloy.

The depth of cut ranged from 3 to 18 mm during the experiments. The tilt angle and skew angle were set to be 0°. Some cutting parameters affecting the performance of conical picks are shown in Fig. 3. According to the geometrical relationship among the relevant angles, the relationships can be expressed as: $\beta = \pi/2 - \phi/2 - \gamma$; $\theta = \gamma - \phi/2$, where β, ϕ and γ are rake angle, cone angle of the pick and attack angle, respectively.

It is noticed that there is no evidence proposing that the cutting speed has a considerable effect on the tool forces and specific energy (Nishimatsu 1972; Bilgin et al. 2006, 2012; Copur et al. 2017). He and Xu (2015) found that the effect of cutting speed on tool forces and specific energy can be ignored if it is assumed to be relatively low (4–20 mm/s). For this reason, the cutting speed is taken to be less than 13 mm/s for all rock-cutting experiments in this study. In addition, the effect of tool wear during rock cutting was eliminated since all cutting tests were carried out using a brand-new pick. The worn pick was replaced with a new one before it suffers obvious wear.

2.2 Effects of Relevant Angles on Cutting Forces

To investigate the effects of relevant angles on cutting force and specific energy, the experiments were carried out at the cutting depth of 6 mm under unrelieved cutting modes on sandstone 1 and sandstone 2. In this context, the attack angle changed from 40° to 60°. The conical picks were produced in the cone angles of 60°, 70°, 80°, 90° and 100°. Accordingly, the rake angle was calculated to be from − 10° to 10°, and the clearance angle changed from 0° to 25°. The experimental results are listed in Table 2.
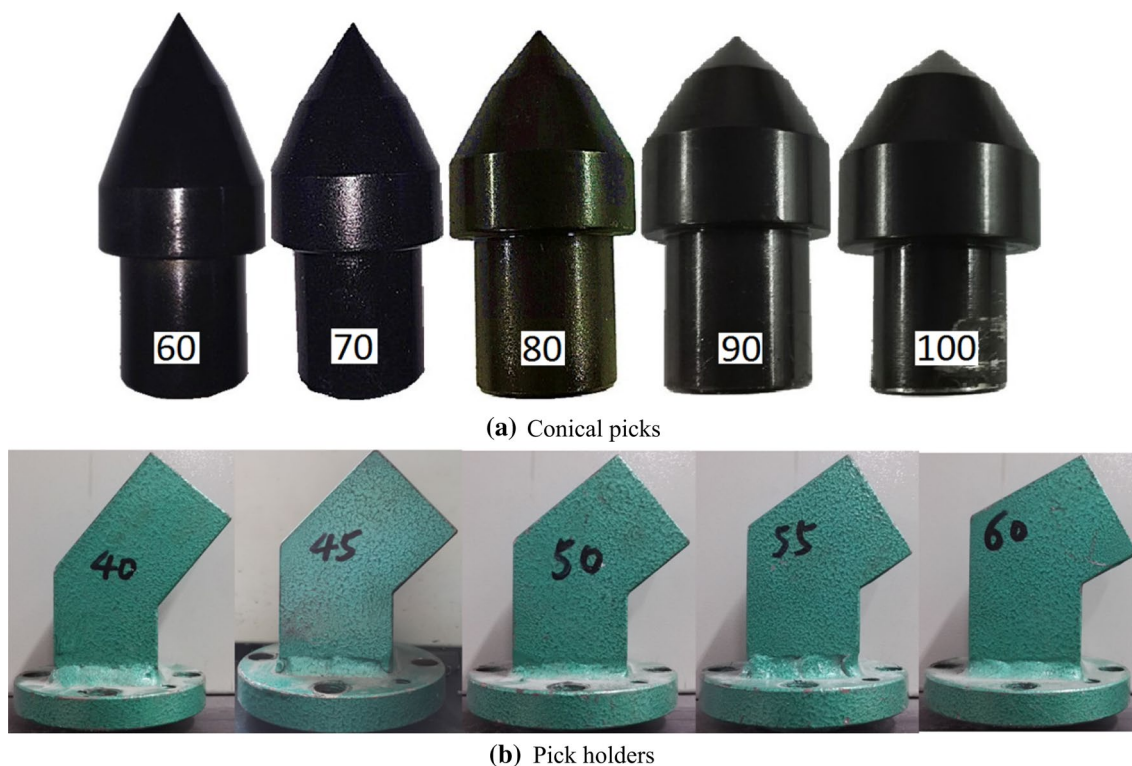

(a) Conical picks

(b) Pick holders

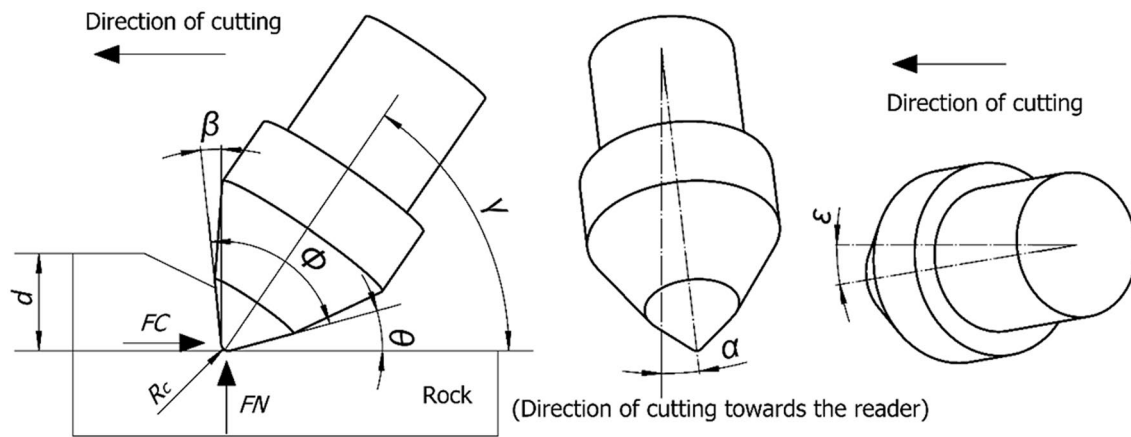**Fig. 2** Conical picks and pick holders used in rock-cutting experiments

Fig. 3 Some of the cutting parameters acting on a conical pick, where FC is the cutting force, FN is the normal force, d is the cutting depth, γ is the attack angle, ϕ is the tip angle, ε is the skew angle, α is the tilt angle, β is the rake angle, θ is the clearance angle

As it is very well known, the specific energy is inversely proportional to the cutting force. Therefore, it is necessary to first discuss the effects of relevant cutting angles on the cutting force based on the test results.

During the cutting tests, if the clearance angle is taken to be very low, serious friction between the pick and rock occurs and it causes the tool forces to dramatically increase (Copur et al. 2017). The relationships between cutting force and clearance angle are shown in Fig. 4. It can be seen that mean cutting force exponentially decreases with increasing clearance angle for sandstone 1 when the clearance angle is lower than 10°. However, mean cutting force increases dramatically due to serious friction between the rock and

the conical tip of the hard permalloy pick when the clearance angle equals to 0°. This finding is also reflected by the characteristics of the cut shown in Fig. 5. As can be seen, the friction surface is wider and smoother in the cut with the clearance angle of 0° (Fig. 5a) compared to the cut where the clearance angle is 15° (Fig. 5b). On the other hand, when the clearance angle is greater than 10°, it seems to have no effect on the mean cutting force for sandstone 1. It can also be observed that no significant correlation was found between the mean cutting force and the clearance angle for sandstone 2 (Fig. 4). However, when the clearance angle is taken to be 5°, it is obvious that the cutting forces are higher than those with clearance angle greater than 5°. Therefore, it is a fact

Table 2 The cutting forces and specific energy under different cutting parameters carried out on sandstone 1 and sandstone 2 ($d=6$ mm)

No.	ϕ (°)	γ (°)	β (°)	θ (°)	Sandstone 1		Sandstone 2	
					FC_m	SE_u	FC_m	SE_u
7055	70	55	0	20	0.74	1.88	2.79	16.99
8050	80	50	0	10	1.04	4.64	2.99	23.95
9045	90	45	0	0	3.39	10.49	–	–
6055	60	55	5	25	0.67	3.16	1.93	13.35
7050	70	50	5	15	0.75	2.24	2.42	11.31
8045	80	45	5	5	2.24	15.96	3.05	56.01
7060	70	60	−5	25	0.99	4.57	3.03	13.79
8055	80	55	−5	15	1.26	6.07	2.66	11.67
9050	90	50	−5	5	2.08	7.72	3.66	39.15
6050	60	50	10	20	0.63	2.91	1.74	14.32
7045	70	45	10	10	1.26	7.10	2.76	33.65
8040	80	40	10	0	3.85	30.69	–	–
8060	80	60	− 10	20	1.29	5.69	3.28	15.93
9055	90	55	− 10	10	1.29	4.25	4.53	19.64
10,050	100	50	− 10	0	4.072	10.04	–	–

ϕ is the tip angle (°), γ is the attack angle (°), β is the rake angle (°), θ is the clearance angle (°), FC_m is the mean cutting force (kN), SE_u is the specific energy in unrelieved cutting mode (kWh/m^3)
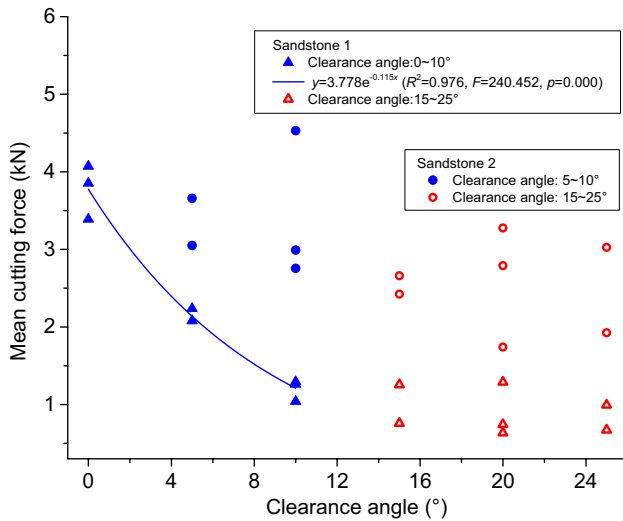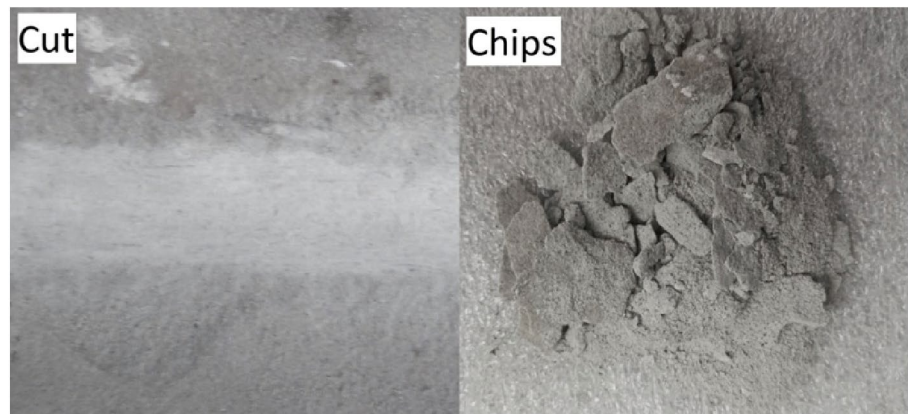
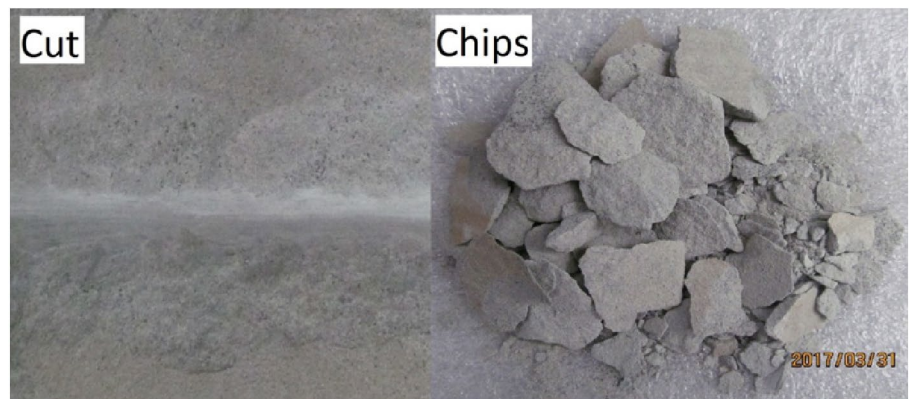**Fig. 4** Relationship between mean cutting force and clearance angle

that the clearance angle has a dominant effect on mean cutting force although the angles higher than 10° were ignored.

Moreover, the relationship between mean cutting force and rake angle based on the test data given in Table 2 is presented in Fig. 6. It can be seen that the cutting force linearly decreases when the rake angle increases. Thus, it can be emphasized that the linear relationship is strong and reliable ($R^2 > 0.8$, $F > 24$, $p < 0.01$) when the clearance angle is greater than 10°.

The relationship between mean cutting force and the cone angle is presented in Fig. 7, which shows that the cutting force increases with the increasing cone angle in power functions for sandstone 1 when the clearance angle is greater than 10°, and for sandstone 2 when the clearance angle is greater than 5°. As it can be seen from Fig. 7, the cutting forces on the picks having the tip angle of 80° increase by approximately 93 and 65% when compared to those having the angle of 60° for sandstone 1 and sandstone 2, respectively.

According to the relationship between relevant angles shown in Fig. 3, the change of attack angle will affect the clearance and rake angles in the same way. The relationship between the mean cutting force and attack angles is provided in Fig. 8, which shows that mean cutting force increases with the increasing attack angle in power function when the clearance angle is greater than 10°. However, it should be noted that the relationships are statistically weak at the confidence level of 90%.
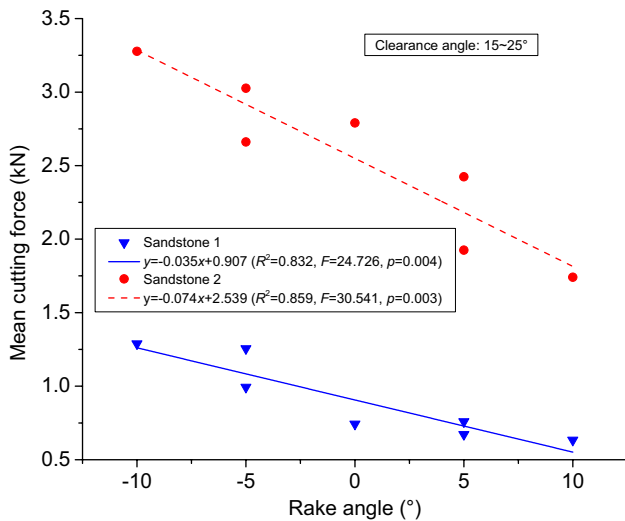
Fig. 5 The cutting surface and rock chips with the cone angle of 80° for sandstone 1

(a) Depth of cut *d*=6 mm, the clearance angle *θ*=0°

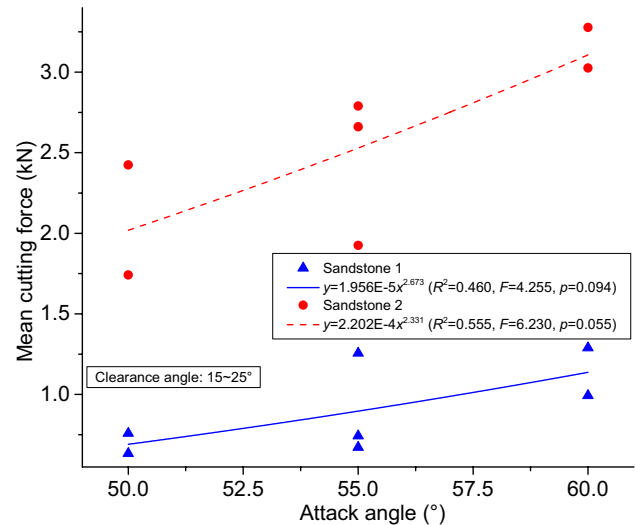**(b)** Depth of cut *d*=6 mm, the clearance angle *θ*=15°

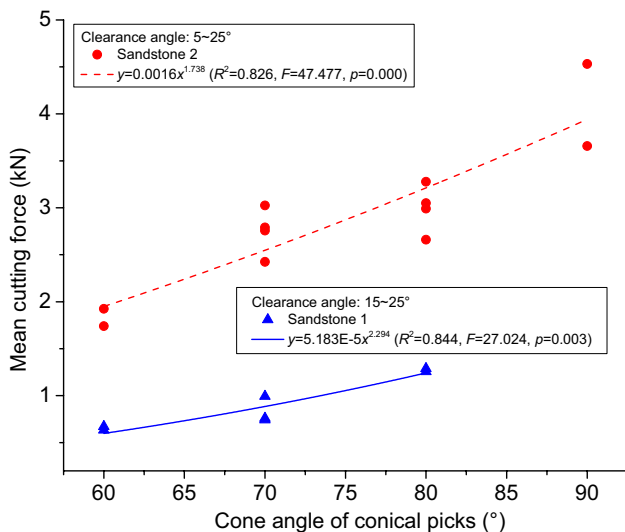**Fig. 6** Relationship between mean cutting force and rake angle

Fig. 7 Relationship between mean cutting force and cone angle for conical picks

2.3 Effects of Relevant Angles on Specific Energy

The correlations between the specific energy and the clearance angle are shown in Fig. 9a, b for sandstone 1 and sandstone 2, respectively. The specific energy exponentially decreases with increasing clearance angle when it is lower than or equal to 10°. The specific energy is very high when the clearance angle is lower than 10°. This is because a wider surface of the conical tip interacts with the rock surface and it causes an increase in friction. Thus, both the cutting force and specific energy increase. On the other hand, it can be seen in Fig. 5 that the rock chips in the clearance angle of 0° are more fragmented than the rock chips in the clearance

Fig. 8 Relationship between mean cutting force and attack angle

angle of 15°, which also means that more specific energy is consumed when a lower value of clearance angle is applied. It should be noted that when the clearance angle is greater than 10° (15°–25°), the specific energy does not vary too much as shown in the histogram of Fig. 9.

In addition, the histograms between the specific energy and the attack angle are shown in Fig. 10a, b for sandstone 1 and sandstone 2, respectively. As seen from the trend lines of these histograms, there is an exponential function when the clearance angle is lower than or equal to 10°. Nevertheless, no significant differences were found in the clearance angle higher than 10°.

Moreover, it is worth noting that there is no statistical relationship among the specific energy, the rake angle and the cone angle of the conical pick.

2.4 Effects of Depth of Cut on Specific Energy

Previous studies have shown that depth of cut has a significant impact on specific energy and dust creation (Fowell and Ochei 1984). Bilgin et al. (2006) showed that variation of specific energy versus depth of cut in unrelieved cutting tests usually approaches asymptotically to a minimum level at the cutting depth greater than 9–10 mm. However, the mathematical relationship between specific energy and depth of cut is still unknown due to limited number of experiments.

In this context, cutting tests were carried out at different depths of cut by applying an 80° cone angle and a 55° attack angle. The skew angle and tilt angle were set to be 0°. The experimental results are summarized in Table 3. Based on the test data, there are strong linear relationships between mean cutting force and depth of cut as expected for all rock samples. This result is consistent with previous
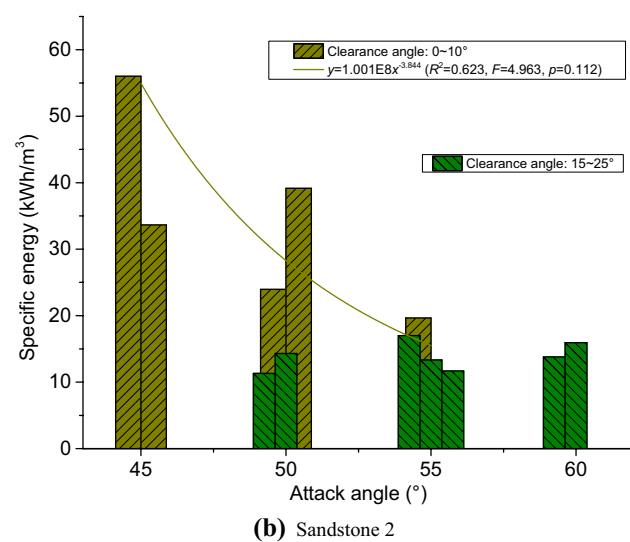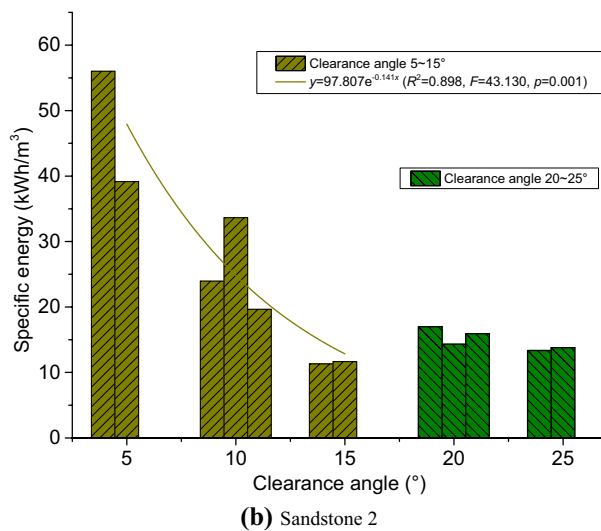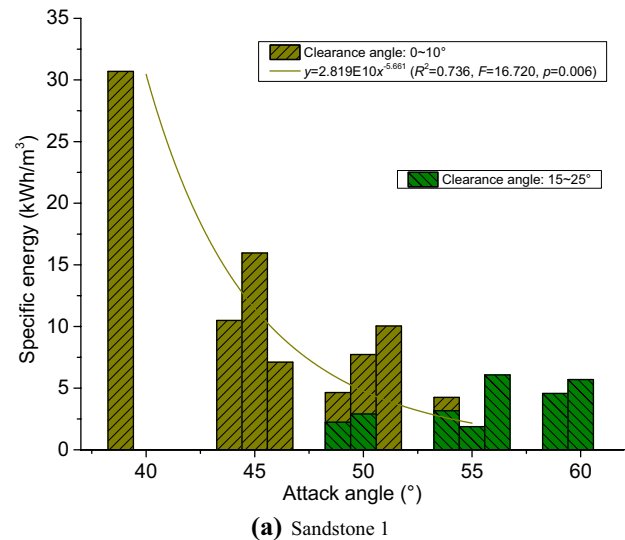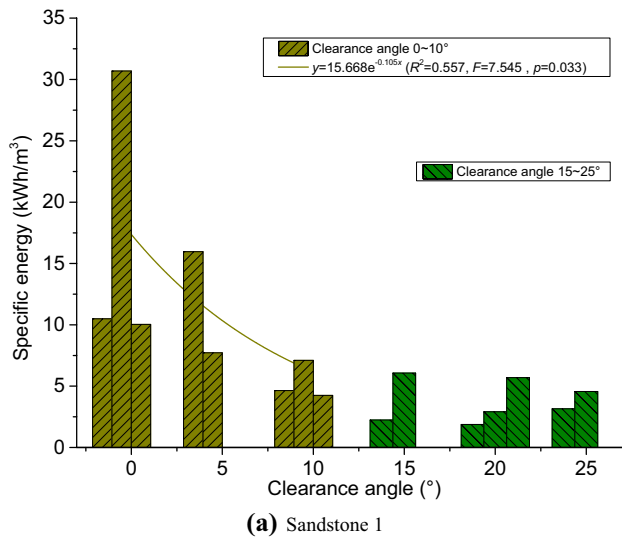
Fig. 9 Relationship between specific energy and clearance angle

Fig. 10 Relationship between specific energy and attack angle for sandstone 1 and sandstone 2

studies by Bilgin et al. (2006) and Shao et al. (2017). The correlations between specific energy and depth of cut are presented in Fig. 11. It can be seen (Fig. 11a) that, with increasing depth of cut, the specific energy in unrelieved cutting decreases with power functions for all rock samples, and the power values of the functions are between -0.850 and -0.620. Figure 11b shows that optimum specific energy also decreases as the depth of cut increases with power functions for sandstone 1 and sandstone 2, whose power values are -0.892 and -0.680, respectively.

2.5 Effects of Relieved Cutting

Rock is excavated by multiple picks mounted on the cutterhead/drum of excavation machines under fixed spacing.

Therefore, relieved cutting is normal in the process of rock cutting. If the cut spacing is too large, the specific energy will be very high. If the cut spacing is too close, the tool forces may be very low, but specific energy will also be high due to over-crushed rock. Previous studies have shown that there should be an optimum ratio of spacing to cutting depth (s/d) to obtain the lowest value of specific energy in the process of rock cutting (Bilgin et al. 2006; Cardu et al. 2017). By combining the data given in Tables 3 and 4, a strong positive correlation, presented in Fig. 12, was found between relieved and unrelieved cutting mode of specific energy ($R^2 = 0.952$, $F = 474.547$, $p = 0.000$). The optimum specific energy is approximately 32.8% lower than the specific energy obtained in unrelieved cutting mode. It should be noted that the ratio of optimum specific energy to specific energy in unrelieved cutting mode, i.e., the slope of the trend

Table 3 Cutting force and specific energy in the process of rock cutting

Method	d	Sandstone 1				Sandstone 2				Sandstone 3		Sandstone 4		Sandstone 5	
		FC_m	SE_u	SE_{opt}	$(s/d)_{opt}$	FC_m	SE_u	SE_{opt}	$(s/d)_{opt}$	FC_m	SE_u	FC_m	SE_u	FC_m	SE_u
Measured	3	0.55	6.47	2.29	3	1.41	29.24	14.80	3	0.93	14.60	0.932	14.05	1.35	10.89
	6	1.26	6.07	1.50	2	2.66	11.67	7.43	2	1.61	7.13	2.369	8.55	2.22	7.72
	9	2.03	3.88	1.35	2	4.11	11.21	5.39	2	3.00	6.02	3.709	5.86	3.27	4.67
	12	2.74	3.40	1.15	3	6.60	8.70	4.31	3	4.60	5.28	5.713	5.82	5.58	3.94
	15	3.42	2.61	–	–	8.25	6.70	–	–	6.22	5.16	8.178	4.84	–	–
	18	4.33	2.25	–	–	–	–	–	–	–	–	–	–	–	–
Equation (3)	3	–	7.39	4.97	–	–	27.18	18.26	–	–	19.11	–	21.25	–	29.21
	6	–	4.20	2.82	–	–	15.43	10.37	–	–	10.85	–	12.06	–	16.58
	9	–	3.01	2.02	–	–	11.08	7.44	–	–	7.79	–	8.66	–	11.90
	12	–	2.38	1.60	–	–	8.76	5.88	–	–	6.16	–	6.85	–	9.41
	15	–	1.98	1.33	–	–	7.30	4.90	–	–	5.13	–	5.71	–	7.84
	18	–	1.71	1.15	–	–	6.29	4.23	–	–	4.42	–	4.92	–	6.76
Equation (4)	3	–	7.96	5.35	–	–	25.13	16.89	–	–	18.35	–	19.70	–	18.45
	6	–	4.43	2.98	–	–	14.00	9.41	–	–	10.22	–	10.97	–	10.28
	9	–	3.15	2.12	–	–	9.94	6.68	–	–	7.26	–	7.79	–	7.30
	12	–	2.47	1.66	–	–	7.80	5.24	–	–	5.70	–	6.11	–	5.73
	15	–	2.05	1.38	–	–	6.46	4.34	–	–	4.72	–	5.06	–	4.74
	18		1.75	1.18	–	–	5.54	3.72	–	–	4.04	–	4.34	–	4.07
Equation (8)	3	–	6.85	4.49	–	–	25.49	17.02	–	–	17.84	–	19.62	–	23.25
	6	–	3.91	2.52	–	–	14.91	9.91	–	–	10.4	–	11.45	–	13.59
	9	–	2.78	1.76	–	–	10.87	7.19	–	–	7.55	–	8.33	–	9.9
	12	–	2.17	1.35	–	–	8.67	5.72	–	–	6.00	–	6.62	–	7.89
	15	–	1.78	1.09	–	–	7.26	4.77	–	–	5.01	–	5.54	–	6.61
	18	–	1.51	0.9	–	–	6.28	4.11	–	–	4.32	–	4.78	–	5.71

d is the depth of cut (mm), FC_m is the mean cutting force (kN), SE_u and SE_{opt} are the specific energy in unrelieved and optimum relieved cutting modes (kWh/m³) and $(s/d)_{opt}$ is optimum ratio of spacing to depth of cut

(0.672), is used to modify the empirical model of specific energy in the following sections.

2.6 Effects of Rock Strength on Specific Energy

Experimental tests have shown that rock strength has a significant influence on the performance of rock cutting with conical picks. Balci et al. (2004) correlated optimum specific energy at 5 and 9 mm depths of cut with the uniaxial compressive and tensile strengths of the rock using power functions based on the test data obtained from full-scale linear rock cutting. Bilgin et al. (2006) suggested there were strong linear relationships between optimum specific energy and the uniaxial compressive strength as well as between optimum specific energy and tensile strengths of the rock. The same finding is also supported by the results of this study.

Based on the test data given in Tables 3 and 4 at the cutting depth of 9 mm, meaningful correlations are found between the specific energy and the uniaxial compressive, as well as between the specific energy and tensile strength of

rock (Fig. 13). It can be seen that linear and power functions give statistically valid relationships of specific energy in unrelieved and optimum relieved cutting mode at the confidence level of 99% ($F = 12.040$–63.895, $p < 0.01$). It is worth noting that the correlations with respect to tensile strength ($R^2 > 0.68$) are slightly superior when compared with those of uniaxial compressive strength ($R^2 > 0.48$).

3 Empirical Models of Specific Energy

3.1 General Models of Specific Energy

By analyzing the effects of relevant cutting parameters and rock strengths on specific energy, the results show that depth of cut and rock strength are the most dominant factors affecting the specific energy. Therefore, general models of specific energy can be expressed as given in Eq. (2):

$$\begin{cases} SE_u = R_\sigma d^{-n} \\ SE_{opt} = k_{opt} SE_u, \end{cases} \qquad (2)$$
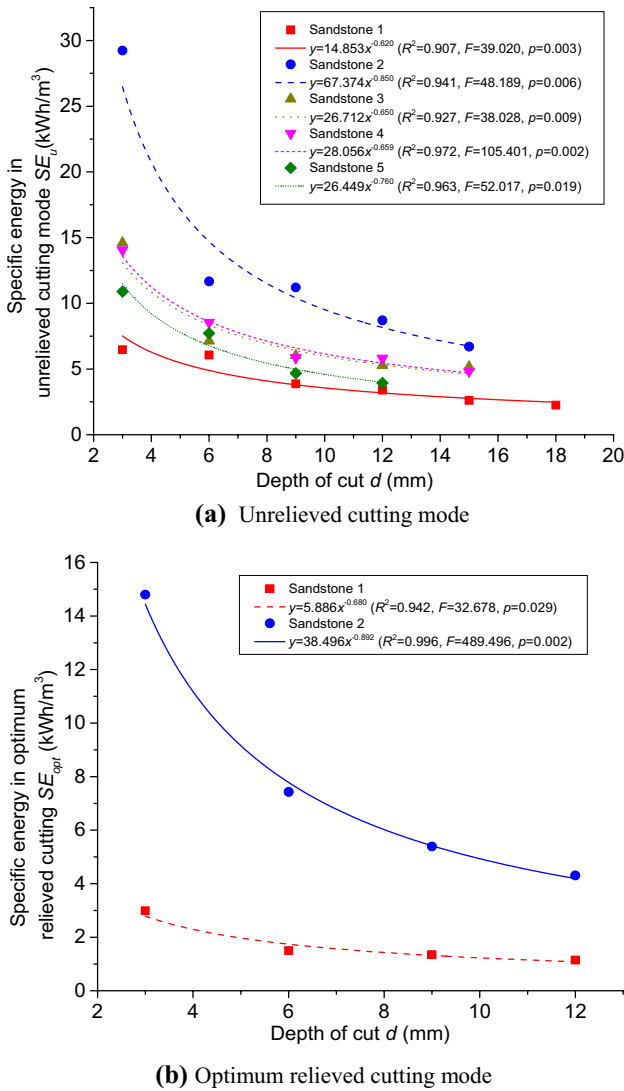
(a) Unrelieved cutting mode

(b) Optimum relieved cutting mode

Fig. 11 Relationship between specific energy and depth of cut

where, SE_u is specific energy in unrelieved mode, SE_{opt} is the optimum specific energy in relieved mode, R_σ is the coefficient representing rock strength parameters, k_{opt} is the ratio of specific energy in relieved to unrelieved cutting mode which was found to be 0.672.

3.2 Empirical Models Based on Multiple Non-linear Regression Method

Based on the study reported in the previous section, the parameter R_σ in Eq. (2) can be expressed by the rock strengths using linear or power functions. The unknown parameters can be obtained by regression analyses based on an appropriate number of experimental data. All regression analyses were carried out with SPSS software. In addition, Levenberg–Marquard Method (L–MM) (Levenberg 1944; Marquardt 1963) was selected for non-linear regression analyses. If only the uniaxial compressive strength or the tensile strength of the rock is to be considered in the regression model, empirical models can be developed as given in Eqs. (3) and (4) by performing the multiple non-linear regression based on the data in Tables 3 and 4. It can be seen that the contribution of each independent variable to the explanation of variation in SE_u models is reasonable in Eqs. (3) and (4). Judging by the coefficients of determination R^2, Eq. (4) ($R^2 = 0.855$) is slightly superior to Eq. (3) ($R^2 = 0.761$).

$$SE_u = 1.448\sigma_c^{0.876}d^{-0.817} \quad (R^2 = 0.761), \tag{3}$$

$$SE_u = 12.044\sigma_t^{1.037}d^{-0.844} \quad (R^2 = 0.855), \tag{4}$$

where, SE_u is the specific energy in unrelieved cutting mode (kWh/m³), σ_c and σ_t are the uniaxial compressive and tensile strengths of rock (MPa), respectively, and d is the depth of cut (mm).

When the uniaxial compressive strength, the tensile strength of rock, and the cutting depth are selected to be independent variables for non-linear regression analyses, the results indicate that the regression equation predicts a decrease in specific energy as the uniaxial compressive strength of the rock increases. This is inconsistent with the previous studies. It is known that σ_c/σ_t is referred as the brittleness index of rock in the literature. Accordingly, the specific energy models can be rewritten as Eq. (5).

$$SE_u = 13.633\sigma_t^{1.039}\left(\frac{\sigma_c}{\sigma_t}\right)^{-0.045}d^{-0.850} \quad (R^2 = 0.856). \tag{5}$$

The cutting force is inversely related to rock brittleness expressed by the ratio (σ_c/σ_t) in the model of Evans (1984). Yagiz (2009) found that measured rock brittleness linearly increased with increasing theoretical values calculated by the ratio (σ_c/σ_t). Copur et al. (2003) proposed that optimum specific energy decreased with a power function with increasing measured rock brittleness values, but no meaningful relations could be found between the specific energy and cutting force and the ratio σ_c/σ_t. Based on the rock cutting tests carried out on a small-scale linear rock cutting machine, Dursun and Gokay (2016) discussed the relations

Table 4 Properties of rocks and the specific energy (kWh/m³) (Copur et al. 2003; Balci et al. 2004; Bilgin et al. 2006)

Rock name	σ_c (MPa)	σ_t (MPa)	Optimum relieved cutting mode								Unrelieved cutting mode											
			SE_{opt5}				SE_{opt9}				SE_3				SE_5				SE_9			
			Mea.	Equation (3)	Equation (4)	Equation (8)	Mea.	Equation (3)	Equation (4)	Equation (8)	Mea.	Equation (3)	Equation (4)	Equation (8)	Mea.	Equation (3)	Equation (4)	Equation (8)	Mea.	Equation (3)	Equation (4)	Equation (8)
High-grade chromite	32	3.7	9.3	5.4	8.1	6.4	3.9	3.4	4.9	4.0	–	12.3	18.5	14.5	11.1	8.1	12.0	9.7	5.8	5.0	7.3	6.1
Medium-grade chromite	47	4.5	12.8	7.6	9.9	8.5	6.4	4.7	6.0	5.3	–	17.2	22.7	19.0	14.8	11.3	14.7	12.8	12.0	7.0	9.0	8.1
Low-grade chromite	46	3.7	10.4	7.5	8.1	7.5	5.0	4.6	4.9	4.7	–	16.9	18.5	16.8	11.7	11.1	12.0	11.3	11.0	6.9	7.3	7.1
Copper ore (yellow)	33	3.4	–	5.6	7.4	6.1	3.7	3.5	4.5	3.8	–	12.6	17.0	13.9	–	8.3	11.0	9.3	–	5.1	6.7	5.8
Copper ore (black)	41	5.7	–	6.8	12.6	9.5	9.2	4.2	7.7	5.9	–	15.3	29.0	21.2	–	10.1	18.8	14.3	–	6.2	11.5	9.0
Harzburgite	58	5.5	14.6	9.2	12.2	10.5	8.4	5.7	7.4	6.6	–	20.7	27.9	23.4	18.6	13.6	18.1	15.8	9.4	8.4	11.0	10.0
Serpentinite	38	5.7	7.0	6.3	12.6	9.2	6.2	3.9	7.7	5.8	–	14.3	29.0	20.7	9.5	9.4	18.8	13.9	8.1	5.8	11.5	8.8
Trona	30	2.2	6.0	5.1	4.7	4.5	2.7	3.2	2.9	2.8	–	11.6	10.8	10.3	8.7	7.7	7.0	6.9	6.7	4.7	4.3	4.3
Anhydrite	82	5.7	–	12.4	12.6	12.5	3.8	7.7	7.7	7.9	–	28.0	29.0	27.8	–	18.5	18.8	18.8	–	11.4	11.5	11.9
Selestite	29	4.0	–	5.0	8.8	6.6	3.0	3.1	5.3	4.1	–	11.3	20.1	14.8	–	7.4	13.0	9.9	–	4.6	7.9	6.2
Jips	33	3.0	–	5.6	6.5	5.7	3.4	3.5	4.0	3.5	–	12.6	14.9	12.8	–	8.3	9.7	8.6	–	5.1	5.9	5.4
Sandstone-1	114	6.6	17.6	16.6	14.7	15.9	12.6	10.2	9.0	10.0	47.2	37.4	33.7	35.4	23.4	24.6	21.9	23.9	13.5	15.2	13.3	15.2
Sandstone-2	174	11.6	–	24.0	26.4	26.3	15.4	14.8	16.1	16.7	54.3	54.2	60.5	58.2	49.6	35.7	39.3	39.3	21.4	22.1	23.9	25.1
Sandstone-3	87	8.3	–	13.1	18.7	16.0	5.4	8.1	11.4	10.1	–	29.5	42.8	35.4	–	19.4	27.8	23.9	–	12.0	16.9	15.2
Siltstone	58	5.3	–	9.2	11.7	10.3	9.6	5.7	7.1	6.4	42.1	20.7	26.9	22.9	24.0	13.6	17.5	15.4	15.5	8.4	10.6	9.7
Limestone	121	7.8	–	17.4	17.5	17.9	12.0	10.8	10.7	11.3	31.7	39.4	40.1	39.7	19.2	26	26.1	26.8	16.4	16.1	15.9	17.0
Tuffite 1	10	1.1	2.3	2.0	2.3	1.7	1.8	1.2	1.4	1.0	–	4.4	5.3	4.2	–	2.9	3.4	2.7	–	1.8	2.1	1.6
Tuffite 2	11	1.4	4.7	2.1	2.9	2.1	3.2	1.3	1.8	1.2	–	4.8	6.8	5.1	–	3.2	4.4	3.4	–	2.0	2.7	2.0
Tuffite 3	27	2.4	4.4	4.7	5.2	4.5	2.6	2.9	3.1	2.8	–	10.6	11.8	10.3	–	7.0	7.7	6.9	–	4.3	4.7	4.3

Table 4 (continued)

| Rock name | σ_c (MPa) | σ_t (MPa) | Optimum relieved cutting mode | | | | | | | | Unrelieved cutting mode | | | | | | | | | | | |
| | | | SE$_{opt5}$ | | | | SE$_{opt9}$ | | | | SE$_3$ | | | | SE$_5$ | | | | SE$_9$ | | | |
			Mea.	Equation (3)	Equation (4)	Equation (8)	Mea.	Equation (3)	Equation (4)	Equation (8)	Mea.	Equation (3)	Equation (4)	Equation (8)	Mea.	Equation (3)	Equation (4)	Equation (8)	Mea.	Equation (3)	Equation (4)	Equation (8)
Tuffite 4	14	1.6	4.3	2.6	3.4	2.6	2.7	1.6	2.1	1.5	–	6.0	7.8	6.1	–	3.9	5.0	4.0	–	2.4	3.1	2.5
Tuffite 5	19	1.3	4.5	3.4	2.7	2.6	2.9	2.1	1.7	1.6	–	7.8	6.3	6.1	-	5.1	4.1	4.1	–	3.2	2.5	2.5
Tuffite 6	6	0.4	1.3	1.3	0.8	0.6	1.3	0.8	0.5	0.3	–	2.8	1.8	1.7	–	1.9	1.2	1.0	–	1.2	0.7	0.5

σ_c and σ_t are the compressive strength and the tensile strength of rock, respectively; *Mea.* is measured specific energy (kWh/m^3); Eqs. (3), (4) and (8) are the calculated specific energies by Eqs. (3), (4), and (8) (kWh/m^3); *d* is depth of cut (mm), SE$_{opt5}$ and SE$_{opt9}$ are optimum cutting energy of 5 mm and 9 mm cutting depth, respectively; SE$_3$ and SE$_5$ are the specific cutting energy in unrelieved cutting modes of 3 mm and 5 mm cutting depth. The cone angle (θ) and attack angle (γ) of the pick used in tests are 80° and 55°, respectively
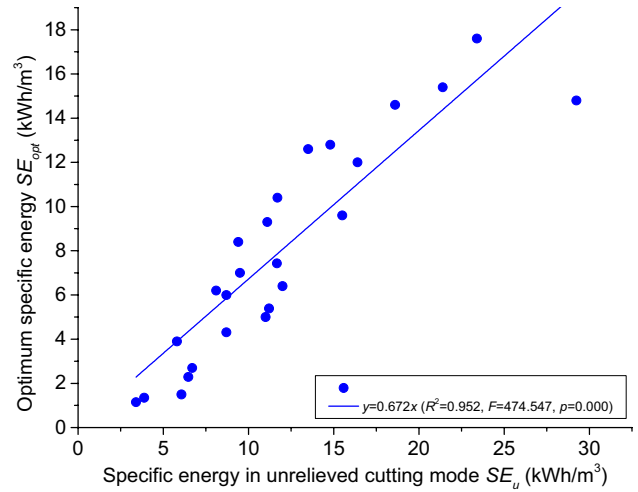
Fig. 12 Relationship between specific energy in optimum relieved cutting mode and unrelieved cutting mode

between all rock brittleness indices and specific energy in detail, whose results indicated that specific energy was proportional to the ratio of σ_c/σ_t. Therefore, the relation between specific energy and the ratio σ_c/σ_t is also controversial based on the available evidence. In this sense, it is important to be very careful while using Eq. (5) for predicting specific energy values although it has a relatively high determination coefficient.

3.3 Empirical Model Based on Principal Component Regression Method

It is worth noting that valid empirical models in Eqs. (3) and (4) include only one type of rock strength based on the multiple non-linear regression method. This is more convenient to use when fewer parameters are included in the model. However, rock is a heterogeneous and anisotropic quasi-brittle material, and its physical and mechanical properties are really discrete. Hence, an empirical model including one type of rock strength sometimes gives unreasonable prediction values. Therefore, it is worth developing a specific energy model considering both the uniaxial compressive and tensile strengths of the rocks. Figure 13a, b show that there are valid relationships between specific energy and rock strength. Thus, the coefficient R_σ can be expressed by a linear combination of the uniaxial compressive and tensile strengths of the rock. The model of specific energy can be written as in Eq. (6).

$$SE_u = (a\sigma_c + b\sigma_t)d^{-n}, \tag{6}$$

where *a* and *b* are unknown coefficients.

According to Eq. (6), when regression analysis is carried out based on the multiple non-linear regression method, the coefficient *a* is still negative according to the existing test
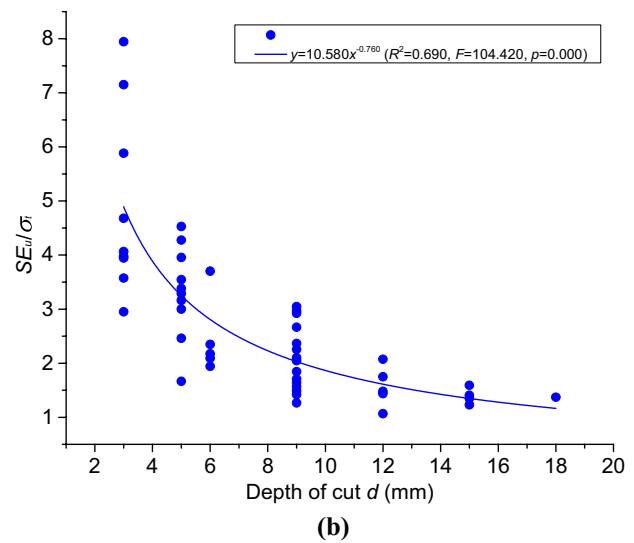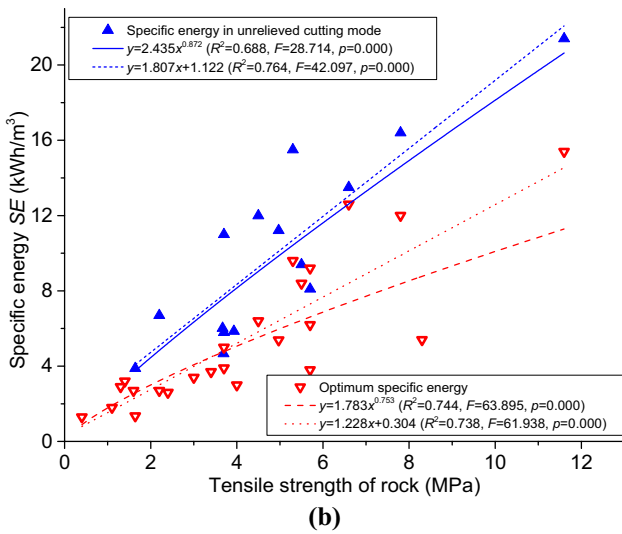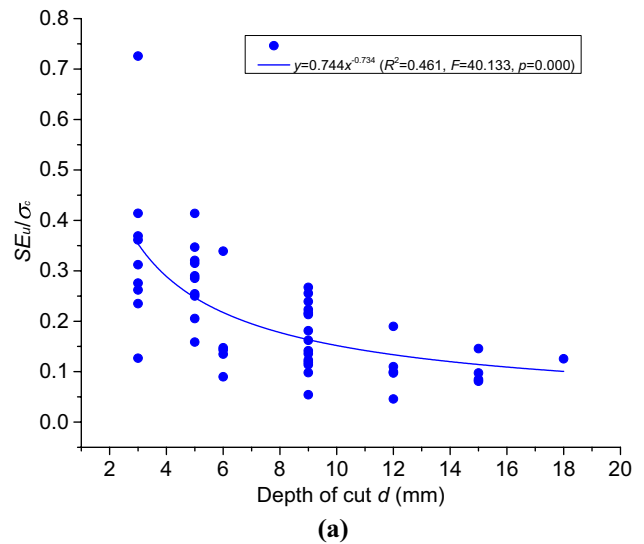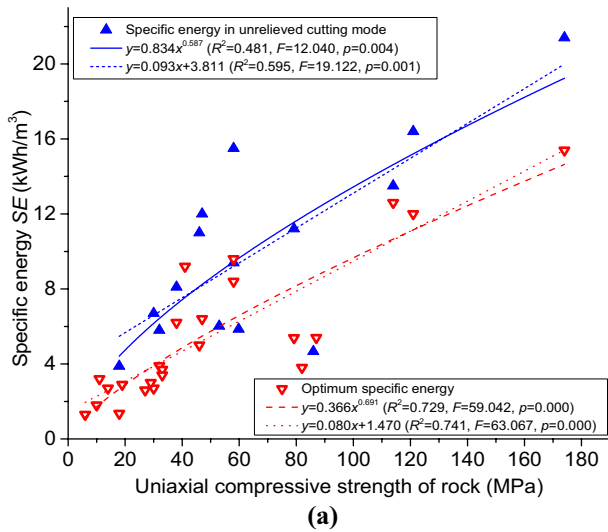
Fig. 13 Relationship between specific energy and rock strength at the cutting depth of 9 mm

Fig. 14 Relationship between SE_u/σ_c, SE_u/σ_t and depth of cut

data, which is inconsistent with the previous studies. For this reason, it is necessary to seek another method to obtain the above unknown coefficients.

In this context, the data were analyzed and the relationships between the SE_u/σ_c ratio and cutting depth, as well as between the ratio of SE_u/σ_t and depth of cut were found (Fig. 14). It can be observed that there are statistically valid relationships between SE_u/σ_c, SE_u/σ_t and depth of cut based on power function fitting. It is worth noting that the power values n of two regression equations are very close to each other ($n = 0.76$ and 0.73). It is interesting to note that the power values of Eqs. (3)–(5) are also very close to each other. Therefore, it can be assumed that the coefficient n is an invariant in Eq. (6) and it is confirmed to be 0.76. Thus, Eq. (6) can be rewritten as in Eq. (7). The problem is transformed by multiple linear regression analysis.

$$SE_u = a_1\sigma_c' + b_1\sigma_t', \tag{7}$$

where a_1 and b_1 are the undetermined coefficients, σ_c' and σ_t' are new variables.

Multiple linear regression analysis is directly carried out using "enter method of regression", and a_1 and b_1 equal -0.104 and 13.662, respectively. It can be seen that contribution of variable σ_c' to the explanation of variation is not reasonable. The variance inflation factors (VIFs) of the variables are respectively: σ_c' (11.243), σ_t' (11.243), which are higher than 10. Figure 15 shows that there is a strong and statistically valid linear relationship between σ_c' and σ_t'. These all indicate that multicollinearity in the regression model is an issue that must be solved (Gunes et al. 2007).

The principal component regression method is an effective method to handle this problem (Wang et al. 2017). One
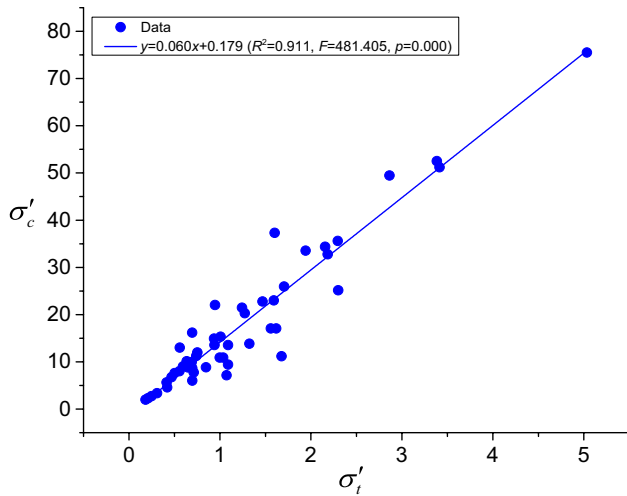
Fig. 15 Relationship between σ_c' and σ_t'

principal component of σ_c' and σ_t' is extracted as a new variable and used for linear regression analyses. Provided that the principal component contains most characteristics of the original variables, the characteristic value and the accumulation contribution rate of the principal component are respectively, 1.954 and 97.725%. In conclusion, an empirical model of specific energy in unrelieved cutting mode can be developed as in Eq. (8).

$$SE_u = (0.3746\sigma_c + 6.005\sigma_t)d^{-0.76} - 0.335 \quad (R^2 = 0.825).$$
(8)

3.4 Validity of Empirical Models

To verify the reliability of the developed specific energy models' given in Eqs. (3), (4) and (8), regression curves were plotted to show the relations between calculated and measured specific energy values for each model, whose results are shown in Fig. 16a for unrelieved cutting and in Fig. 16b for optimum relieved cutting, respectively. It should be noted that Eq. (5) was omitted due to confusing results. The relevant regression equations are listed in Table 5. Accordingly, it is found that there are statistically significant relations between calculated and measured specific energy values derived from Eqs. (3), (4) and (8) in unrelieved mode ($R^2 = 0.762$–0.855) at the confidence level of 99% ($F = 150.230$–278.010, $p = 0.000$) (Fig. 16a). In addition, it can be apparently seen that data points are all evenly distributed over, above and below the line of $y = x$ without any outlying points. On the other hand, the determination coefficient R^2 statistics indicate that the models reveal more than 76% of the variability in the calculated specific energy values in unrelieved mode. The correlation coefficients R yielded by Eqs. (3), (4) and (8) are more than 0.87 provided that strong relationships exist between variables.
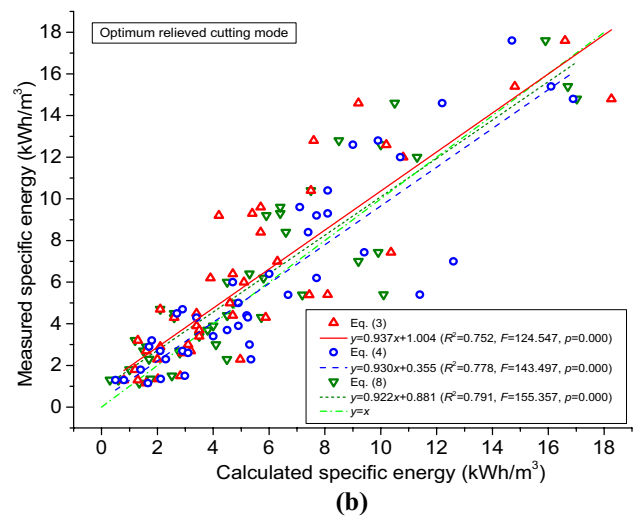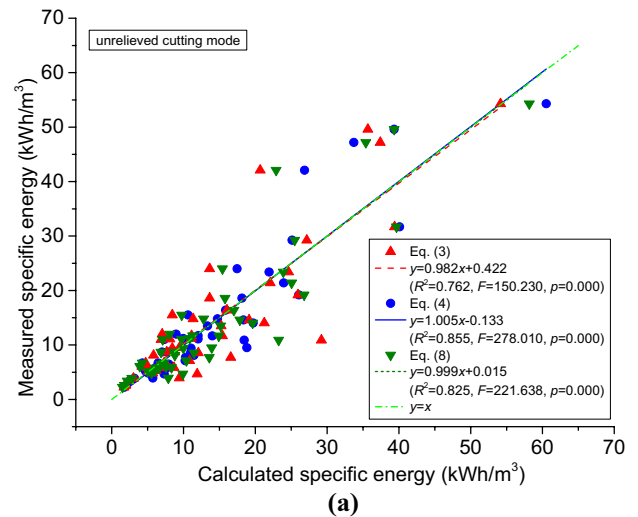

Fig. 16 Relationship between measured and calculated specific energy by different models

Figure 16b shows that the optimum specific energy can also be satisfactorily predicted by Eqs. (3), (4) and (8) with the modified factor k_{opt} ($R^2 = 0.752$–0.791, $F = 124.547$-155.357, $p = 0.000$), although the validity is slightly less powerful than that of the unrelieved mode.

Furthermore, the student t test was carried out to see whether the calculated specific energy values were significantly different from the measured ones. The results listed in Table 5 show that there is no significant difference between calculated and measured specific energy, both in unrelieved and optimum relieved cutting modes at the 95% confidence level, as the p values of t are all greater than 0.05. For further comparison of the performance of the models, the variance account for (VAF) and the root mean square error (RMSE) were calculated, and the results are summarized in Table 5. The interpretation of VAF and RMSE performance indices is as follows: the higher VAF, the better model performs; the

Table 5 Relationship between measured and calculated specific energy by different models and related statistical parameters at $\alpha = 0.05$ level

Cutting mode	Calculated model	Regression equation	R^2	F value	p value	t value	p value	VAF (%)	RMSE
Unrelieved cutting	Equation (3)	$y = 0.982x + 0.422$	0.762	150.230	0.000	0.430	0.688	76.14	5.98
	Equation (4)	$y = 1.005x - 0.133$	0.855	278.010	0.000	0.099	0.921	85.54	4.65
	Equation (8)	$y = 0.999x + 0.015$	0.825	221.638	0.000	0.236	0.814	82.50	5.11
Optimum relieved cutting	Equation (3)	$y = 0.937x + 1.004$	0.752	124.547	0.000	0.725	0.471	74.90	2.275
	Equation (4)	$y = 0.930x + 0.355$	0.778	143.497	0.000	-0.081	0.936	77.34	2.070
	Equation (8)	$y = 0.922x + 0.881$	0.791	155.351	0.000	0.468	0.641	78.55	2.059

lower RMSE, the better model performs (Gunes et al. 2007). Therefore, the values of VAF and RMSE listed in Table 5 show that the performance of Eq. (3) is slightly poorer than those of Eqs. (4) and (8).

Therefore, all statistical analyses indicate that Eqs. (3), (4) and (8) can all be used for effectively predicting the specific energy at different levels of cutting depth for rock samples. In general, the fewer the parameters used in the models, the better is their economic benefit. Based on this consideration, Eqs. (3) and (4) would be more convenient than Eq. (8). However, considering rock strengths, the prediction performance of the model may be more stable. Therefore, Eq. (8) is also highly recommended. In conclusion, all empirical models and modified factors of specific energy are summarized in Table 6.

4 Production Assessment of Roadheader Based on Specific Energy

4.1 Available Model of Roadheader Production Rate

The prediction of instantaneous (net) cutting rate (ICR or NCR) is very important while selecting an actual machine and planning the schedule of tunneling projects (Bilgin et al. 2005). Many studies have been carried out so far to predict the instantaneous cutting rate, which is defined as the production rate during a continuous excavation phase. Gehring (1989) and Thuro and Plinninger (1999) suggested that the compressive strength of rock is the main factor affecting the production of roadheaders. Bilgin et al. (1990) proposed an empirical model to predict the production rate of roadheaders by taking the compressive strength of rock and rock quality designation into account. Field data analyses showed that some geological and geotechnical factors also have remarkable influences on the performance of roadheaders (Bilgin et al. 2004). Rostami et al. (1994) developed a model to predict the instantaneous cutting rate of them using optimum specific cutting energy as given in Eq. (9), which has widely been praised by the industry and used for predicting the performance of roadheaders (Balci et al. 2004; Bilgin et al. 2005; Tumac et al. 2007; Comakli et al. 2014). Based on field data, Avunduk et al. (2014) predicted roadheader production through artificial neural networks by considering the uniaxial compressive strength and rock quality designation as inputs. The results indicated that it had a better prediction performance than the empirical models.

$$\mathrm{ICR} = k\frac{P}{\mathrm{SE_{opt}}}, \tag{9}$$

Table 6 Empirical prediction models of specific energy and production of roadheaders

Known rock strength	Specific energy (SE)	Production rate of roadheaders (ICR)
The uniaxial compressive strength (σ_c)	$\begin{cases} \mathrm{SE}_u = 1.448\sigma_c^{0.876}d^{-0.817} \ (R^2 = 0.761) \\ \mathrm{SE_{opt}} = k_{opt}\mathrm{SE}_u \end{cases}$ $k_{\mathrm{opt}} = 0.672$	$\mathrm{ICR} = 1.028kP\sigma_c^{-0.876}d^{0.817}$ $k = 0.45 - 0.55$
The tensile strength (σ_t)	$\begin{cases} \mathrm{SE}_u = 12.044\sigma_t^{1.037}d^{-0.844} \ (R^2 = 0.855) \\ \mathrm{SE_{opt}} = k_{opt}\mathrm{SE}_u \end{cases}$	$\mathrm{ICR} = 0.124kP\sigma_t^{-1.037}d^{0.844}$
The uniaxial compressive and tensile strengths (σ_c and σ_t)	$\begin{cases} \mathrm{SE}_u = (0.3746\sigma_c + 6.005\sigma_t)d^{-0.76} - 0.335\,(R^2 = 0.825) \\ \mathrm{SE_{opt}} = k_{opt}\mathrm{SE}_u \end{cases}$	$\mathrm{ICR} = \dfrac{kP}{(0.253\sigma_c + 4.035\sigma_t)d^{-0.76} - 0.335}$

SE_u and SE_{opt} are specific energy in unrelieved cutting mode and in optimum relieved mode (kWh/m^3) respectively, d is depth of cut (mm), k_{opt} is the ratio of optimum specific energy to specific energy in unrelieved cutting mode, ICR is the instantaneous cutting rate of the roadheader (m^3/h), P is cutting power of cutting head (kW) and k is the energy transfer ratio

where ICR is the instantaneous cutting rate (m³/h), P is the cutting power of the cutting head (kW), and k is the energy transfer ratio (0.45–0.55 for roadheaders).

Based on Eqs. (3), (4), (8) and (9), prediction models of roadheader production rate can be proposed as given in Eqs. (10)–(12) in Table 6.

$$\text{ICR} = 1.028kP\sigma_c^{-0.876}d^{0.817}, \tag{10}$$

$$\text{ICR} = 0.124kP\sigma_t^{-1.037}d^{0.844}, \tag{11}$$

$$\text{ICR} = \frac{kP}{(0.253\sigma_c + 4.035\sigma_t)d^{-0.76} - 0.335}. \tag{12}$$

It should be noted that the ICR of roadheaders is closely related to the cutting depth. That is supported by the previous study of Origliasso et al. (2014) for surface miners. It can also be seen that one or two types of rock strengths are involved in Eqs. (10–12), and therefore, it is suggested that engineers choose the appropriate model in the light of available parameters. If both the uniaxial compressive and tensile strengths are known, the minimum values of Eqs. (10–12) can be chosen as the final result based on all these proper considerations.

4.2 Validity of Proposed Models

According to the studies of Bilgin et al. (2005) and Tumac et al. (2007), a SM1 shielded Herrenknecht roadheader was used in a sewage tunnel (Kucuksu-Istanbul). The cutting power and total power of the roadheader were 90 and 224 kW, respectively. The cutting head was an axial type containing 36 conical picks with the cone angle of 75°. In this context, the validity of Eq. (10) was examined to predict the ICR of the roadheader, the results of which are listed in Table 7. It should be noticed that the factor k is set to be 0.45 in Eq. (10).

To determine whether the measured ICR values were significantly different from the predicted values, the student t test was carried out. The results of t test listed in Table 7 indicate that the predicted *ICR* values at 6 and 10 mm of cutting depth are significantly different from the measured values at the confidence level of 95% due to having the p values of t values lower than 0.05. Nevertheless, there is no significant difference between the measured and the predicted ICR values at the cutting depth of 7, 8, and 9 mm.

The relations between measured and predicted ICR at 6, 8, 10 mm depth of cut are presented in Fig. 17. It can be seen that there are strong and statistically linear relationships

Table 7 Rock properties, instantaneous (net) cutting rates and related statistical parameters at $\alpha = 0.05$ level (Tumac et al. 2007)

Rock	σ_c	ICR_6	ICR_7	ICR_8	ICR_9	ICR_{10}	ICR_m
Sandstone	55.7	5.32	6.03	6.73	7.41	8.07	6.85
Limestone	98.2	3.24	3.67	4.09	4.51	4.91	4.36
Siltstone	92.4	3.41	3.87	4.32	4.75	5.18	3.6
Limestone	122.7	2.66	3.02	3.37	3.71	4.04	3
Limestone	95.7	3.31	3.76	4.19	4.61	5.03	3.52
Limestone	120.4	2.71	3.07	3.42	3.77	4.11	2.68
Limestone	127.8	2.57	2.91	3.25	3.58	3.90	3.3
Andesite	163.8	2.07	2.35	2.62	2.88	3.14	3.45
Limestone	145.2	2.30	2.61	2.91	3.20	3.49	3.33
Limestone	120.5	2.71	3.07	3.42	3.77	4.11	3.55
Siltstone	82.6	3.77	4.27	4.76	5.25	5.72	4.1
Limestone	116.4	2.79	3.16	3.53	3.88	4.23	3.33
Diabase	77	4.01	4.54	5.07	5.58	6.08	4.94
Siltstone	75	4.10	4.65	5.18	5.71	6.22	5.1
Sandstone	75	4.10	4.65	5.18	5.71	6.22	5
d (mm)	6		7	8	9	10	–
Statistical results							
t value	2.061		0.791	− 0.325	− 1.307	− 2.176	–
p value	0.049		0.435	0.748	0.202	0.038	–
VAF	82.02%		83.23%	82.25%	79.09%	74.01%	–
RMSE	0.8591		0.5219	0.4586	0.7266	1.0944	–

t value and p value are statistical parameters of student t test. ICR_6, ICR_7, ICR_8, ICR_9 and ICR_{10} are the predicted instantaneous cutting rate (m³/h) at the cutting depth of 6, 7, 8, 9 and 10 mm, respectively

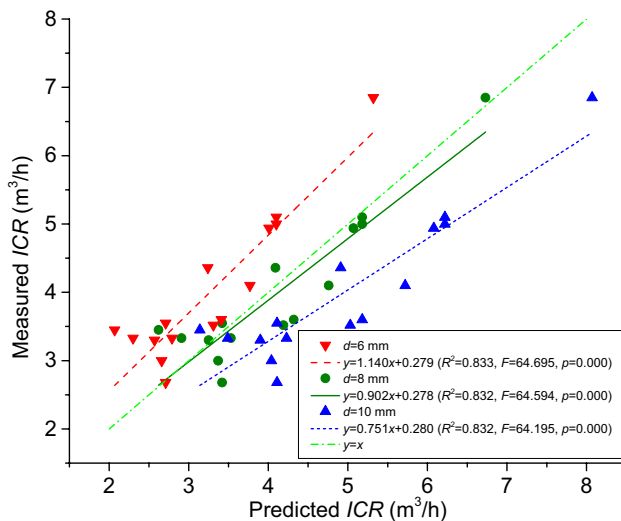ICR_m is the measured instantaneous cutting rate (m³/h)

between measured and predicted *ICR*. On the basis of the relative position of the regression lines and line of *y = x*, the predicted ICR is over-estimated when the depth of cut is 10 mm. However, when the depth of cut is taken to be 6 mm, the predicted ICR is under-estimated. When it is 8 mm, the predicted values are very close to the measured values. The results are also supported by the values of VAF and RMSE listed in Table 7.

5 Conclusions

Specific energy is a significant factor affecting the rock cutting efficiency and it is closely related to the rock properties as well as relevant cutting parameters. Experimental results have indicated that the clearance angle has an important influence on the cutting force and specific energy when it is relatively low because the friction can dramatically increase the cutting force acting on the conical pick. When the clearance angle is greater than 10°, the cutting force linearly increases with the increasing cone angle of the conical pick and linearly decreases with increasing rake angle. However, the clearance angle has a weak impact on the specific energy when it is greater than 10°. In addition, there is no statistical relationship between specific energy and relevant angles, e.g., the attack angle, the cone angle, and the rake angle. Statistical analysis shows that the cutting force linearly increases with the increasing depth of cut, and the specific energy decreases as a power function while the depth of cut increases. Furthermore, linear and power functions can all be used for efficiently expressing the statistical relations between specific energy and the compressive and tensile strengths of the rock.

Following the analyses of all critical cutting parameters, a general empirical model of specific energy was proposed by considering the rock strength and depth of cut. Based on the test data from the present and previous studies, multiple non-linear regression and principal component regression methods were used to develop empirical models of specific energy. Besides rock strength, the depth of cut was also taken into account. The performance of the proposed models was evaluated using statistical correlation and *t* test, and agreement exists between the measured and predicted specific energy values in unrelieved and optimum relieved cutting modes. It should be noted that the empirical models have a very wide range of applications for different rocks since the rock and ore samples used for regression analysis have uniaxial compressive strengths varying from 6 to 174 MPa. However, it can be emphasized that the empirical models of specific energy in the present study should be used carefully when the clearance angle is very low.

Based on the model of Rostami et al. (1994) for evaluating the production rate of roadheaders, three empirical additional prediction models are proposed. Statistical analyses indicated that these models have a good performance when the depth of cut varies between 7 and 9 mm.

References

Avunduk E, Tumac D, Atalay AK (2014) Prediction of roadheader performance by artificial neural network. Tunn Undergr Space Technol 44:3–9

Balci C, Bilgin N (2007) Correlative study of linear small and full-scale rock cutting tests to select mechanized excavation machines. Int J Rock Mech Min Sci 44:468–476

Balci C, Demircin MA, Copur H, Tuncdemir H (2004) Estimation of optimum specific energy based on rock properties for assessment of roadheader performance. J S Afr Inst Min Metall 104(11):633–642

Bilgin N, Seyrek T, Erdinc E, Shahriar K (1990) Roadheaders glean valuable tips for Istanbul Metro. Tunnels Tunnell October 29–32

Bilgin N, Dincer T, Copur H, Erdogan M (2004) Some geological and geotechnical factors affecting the performance of a roadheader in an inclined tunnel. Tunn Undergr Space Technol 19:629–636

Bilgin N, Dumac D, Feridunoglu C, Karakas AR, Akgul M (2005) The performance of a roadheader in high strength rock formations in Kücüksu tunnel. In: Proceedings of the 31st ITA-AITES World Tunnel Congress. Istanbul, pp 815–820

Bilgin N, Demircin MA, Copur H, Balci C, Tuncdemir H, Akcin N (2006) Dominant rock properties affecting the performance of

conical picks and the comparison of some experimental and theoretical results. Int J Rock Mech Min Sci 43:139–156

Bilgin N, Copur H, Balci C (2012) Effect of replacing disc cutters with chisel tools on performance of a TBM in difficult ground conditions. Tunn Undergr Space Technol 27:41–51

Bilgin N, Copur H, Balci C (2014) Mechanical excavation in mining and civil industries CRC Press, Boca Raton, p p366

Brown TT (ed) (1981) ISRM suggested methods. Rock characterization testing and monitoring. Pergamon Press, Oxford, 211 p ISRM

Cardu M, Iabichino G, Oreste P, Rispoli A (2017) Experimental and analytical studies of the parameters influencing the action of TBM disc tools in tunneling. Acta Geotech. https://doi.org/10.1007/s11440-016-0453-9

Comakli R, Kahraman S, Balci C (2014) Performance prediction of roadheaders in metallic ore excavation. Tunn Undergr Space Technol 40:38–45

Copur H, Bilgin N, Tuncdemir H, Balci C (2003) A set of indices based on indentation tests for assessment of rock cutting performance and rock properties. J S Afr Inst Min Metall 103(11):589–599

Copur H, Bilgin N, Balci C, Tumac D, Avunduk E (2017) Effects of different cutting patterns and experimental conditions on the performance of a conical drag tool. Rock Mech Rock Eng. https://doi.org/10.1007/s00603-017-1172-8

Dursun AE, Gokay MK (2016) Cuttability assessment of selected rocks through different brittleness values. Rock Mech Rock Eng 49(4):1173–1190

Evans I (1984) A theory of the cutting force for point-attack picks. Int J Min Eng 2:63–71

Fowell RJ, Ochei NN (1984) A comparison of dust make and energy requirements for rock cutting tools. Int J Min Eng 2:73–83

Gehring KH (1989) Cutting comparison. Tunn Tunn Int 21(11): 27–30

Gunes N, Yurdakul M, Goktan RM (2007) Prediction of radial bit cutting force in high-strength rocks using multiple linear regression analysis. Int J Rock Mech Min Sci 44:962–970

Gunes N, Tumac D, Goktan RM (2014) Rock cuttability assessment using the concept of hybrid dynamic hardness (HDH). Bull Eng Geol Environ 74(4):1–12

He X, Xu C (2016) Specific energy as an index to identify the critical failure mode transition depth of rock cutting. Rock Mech Rock Eng 49(4):1461–1478

Hughes H (1972) Some aspects of rock machining. Int J Rock Mech Min Sci 9:205–211

Hurt KG, Evans I (1981) Point attack tools: an evaluation of function and use for rock cutting. Min Eng 140:673–675

Hurt KG, McAndrew KM (1985) Cutting efficiency and life of rock cutting picks. Min Sci Technol 2:139–151

Levenberg K (1944) A method for the solution of certain non-linear problems in least squares. J Heart Lung Transpl 2(4):436–438

Marquardt DW (1963) An algorithm for least square estimation of non-linear parameters. J Soc Ind Appl Math 11(2):431–441

Mellor M (1972) Normalization of specific energy values. Int J Rock Mech Min Sci 9:661–663

Nishimatsu Y (1972) The mechanics of the rock cutting. Int J Rock Mech Min Sci 9:261–270

Origliasso C, Cardu M, Kecojevic V (2014) Surface miners: evaluation of the production rate and cutting performance based on rock properties and specific energy. Rock Mech Rock Eng 47(2):757–770

Rostami J, Ozdemir L, Neil DM (1994) Performance prediction: a key issue in mechanical hard rock mining. Min Eng 46(11):1264–1267

Shao W, Li XS, Sun Y, Huang H (2017) Parametric study of rock cutting with SMART*CUT picks. Tunn Undergr Space Technol 62:134–144

Thuro K, Plinninger RJ (1999) Predicting roadheader advance rates. Tunn Tunnel 6:36–39

Tiryaki B (2009) Estimating rock cuttability using regression trees and artificial neural networks. Rock Mech Rock Eng 42(6):939–946

Tiryaki B, Dikmen AC (2006) Effects of rock properties on specific cutting energy in linear cutting of sandstones by picks. Rock Mech Rock Eng 39(2):89–120

Tumac D, Bilgin N, Feridunoglu C, Ergin H (2007) Estimation of rock cuttability from shore hardness and compressive strength properties. Rock Mech Rock Eng 40(5):477–490

Wang X, Liang YP, Wang QF, Zhang ZY (2017) Empirical models for tool forces prediction of drag-typed picks based on principal component regression and ridge regression methods. Tunn Undergr Space Technol 62:75–95

Yagiz S (2009) Assessment of brittleness using rock strength and density with punch penetration test. Tunnel Undergr Space Technol 24:66–74

Yurdakul M, Gopalakrishnan K, Akdas H (2014) Prediction of specific cutting energy in natural stone cutting processes using the neuro-fuzzy methodology. Int J Rock Mech Min Sci 67:127–135